Journal of Research in Forestry, Wildlife & Environment Vol. 15(2) June, 2023
E-mail: *jrfwe2019@gmail.com; jfewr@yahoo.com*
http://www.ajol.info/index.php/jrfwe

jfewr ©2023 - jfewr Publications
ISBN: 2141 – 1778

EXPLORING THE GEOCHEMISTRY OF GOLD MINERALIZATION IN TOTO LOCAL GOVERNMENT AREA, NASARAWA STATE, NIGERIA

***[1]Sylvanus, H. B. and [1]Muhammad, Q. H.**

Department of Geography, Nigerian Defence Academy (NDA), Kaduna, Nigeria
***Corresponding Author:** *heldabernard@gmail.com;* +234 803 058 2272

ABSTRACT

This study explores the geochemistry of gold mineralization in Toto Local Government Area, Nasarawa State Nigeria. The study utilized field and remote sensing data which includes field sampled soil, rocks, Landsat-7 ETM+ and ASTER DEM which were used to detect alterations, extraction and characterization of lineaments associated with gold deposits. The analysis dealt with Oxide composition in percentages which were reclassified into Sio2, Tio2, Al2o3, Fe2o3, Cao amongst others. These were carried out in a GIS working environment using the ArcGIS Software. Results from the Geochemical Analysis (KXRF analysis) show that the sample ST1A, ST3, ST04, STV10, GL01, GL02, GL03, VRII S2, STO4, STVS9, HNVS1 in most profiles generally have the highest concentration (response) of key pathfinder elements (As, Cu, Pb, Zn, Mn). Assessment of the geochemical data indicates that Fe (iron oxide/ox hydroxide) has an important influence on pathfinder element geochemistry in the study area samples. This is indicated by moderate to strong positive correlation between Fe and the elements in the total data set and the individual profile distribution patterns. Result from the study also shows that arsenic generally shows a selective concentration in some samples which happens to be a major pathfinder of Au mineralization followed by copper which is probably the most useful of the major pathfinder elements. The study therefore concludes that based on the outcome of the field sampled rocks, gold mineralization in Toto area is dispersed spatially and geochemically which is attributed to pathfinder. Hence recommends for drilling operations in order to uncover the vertical geochemistry and minerals concentrate with depth of the area using the GIS and remote sensing data/technique.

Keywords: Geochemistry, Mineralization, Drilling, Nasarawa State Nigeria, Resource, Remote Sensing

Correct Citation of this Publication
Sylvanus, H. B. and [1]Muhammad, Q. H. (2023). Exploring the Geochemistry of Gold Mineralization in Toto Local Government Area, Nasarawa State, Nigeria. *Journal of Research in Forestry, Wildlife & Environment* Vol. 15(2): 288 – 301.

INTRODUCTION

Geochemistry plays a crucial role in mineral exploration, aiding in the identification and evaluation of potential mineral deposits. It involves the study of the chemical composition, distribution, and behavior of elements and compounds in rocks, soils, sediments, and water. By analyzing geochemical data, geoscientists can infer the presence and concentration of specific elements associated with mineralization, helping to guide exploration efforts. The escalating demand for minerals, driven by the need to supply various industries with raw materials and diversify national income sources, has led to an increased emphasis on exploration (Oyinloye and Oyinloye, 2017). This surge in exploration activities is particularly evident across numerous regions in Nigeria.

The abundant mineral resources in Nasarawa state encompassing a wide range of solid minerals found in the Nigerian geological environment. The region is particularly rich in various types of minerals which includes barite, muscovite, limestone, micas, and glass sand, Metallic minerals such as lead-zinc, wolframite, columbite-cassiterite, tantalite, and

iron ore are also present. The geological history of the region indicates that gold mineralization occurs within the structures that intrude the basement complex rocks, following a N-S trending pattern (strike) (Okonkwo and Dada, 2020). Additionally, semi-precious minerals like tourmaline, beryl, aquamarine, and topaz, as well as evaporates like brine, and precious minerals such as ruby, can be found in the area (Okonkwo and Dada, 2020).

In spite of the abundant mineral resources, particularly in the Toto area of Nasarawa state, it is regrettable that these valuable assets remain largely untapped. This untapped potential signifies a missed opportunity for economic growth and development in the region. A significant obstacle impeding the exploitation of these mineral resources is the absence of technical expertise and knowledge within the area. Successful mining operations necessitate specialized skills, scientific expertise, and appropriate regulatory frameworks to ensure sustainable and responsible extraction practices. Without the requisite knowledge and trained professionals, the local population may encounter difficulties in effectively capitalizing on these resources.

This study therefore, explores the geochemistry of mineral resources in the study area by identifying the geochemical signatures and spatial patterns of gold and how they relate to the tectonic and magmatic evolution of the area. The research uses a combination of field sampling, laboratory analysis, and geostatistical modelling to characterize the gold-bearing rocks and fluids to map their distribution and variability in Toto LGA. The research also compares and contrast the geochemical features of gold mineralization in Toto LGA with those of other gold provinces in Nigeria and West Africa. The research will contribute to the understanding of the origin and evolution of gold deposits in Toto LGA and to the development of effective exploration and mining strategies for the area.

MATERIALS AND METHODS

The Study Area

Toto LGA is located between Latitudes 08° 07′ 13″N and 8° 23′ 11″North of the Equator and Longitudes 7° 11′ 04″E and 7° 18′ 01″East of Greenwich Meridian. The area has a landmass of about 2,903 km^2 at an average elevation of 145m above sea level. The local government area is bounded to the north by the Federal Capital Territory, to the east by Nasarawa local government area, and to the south and west by Kogi State as shown in Figure 1.

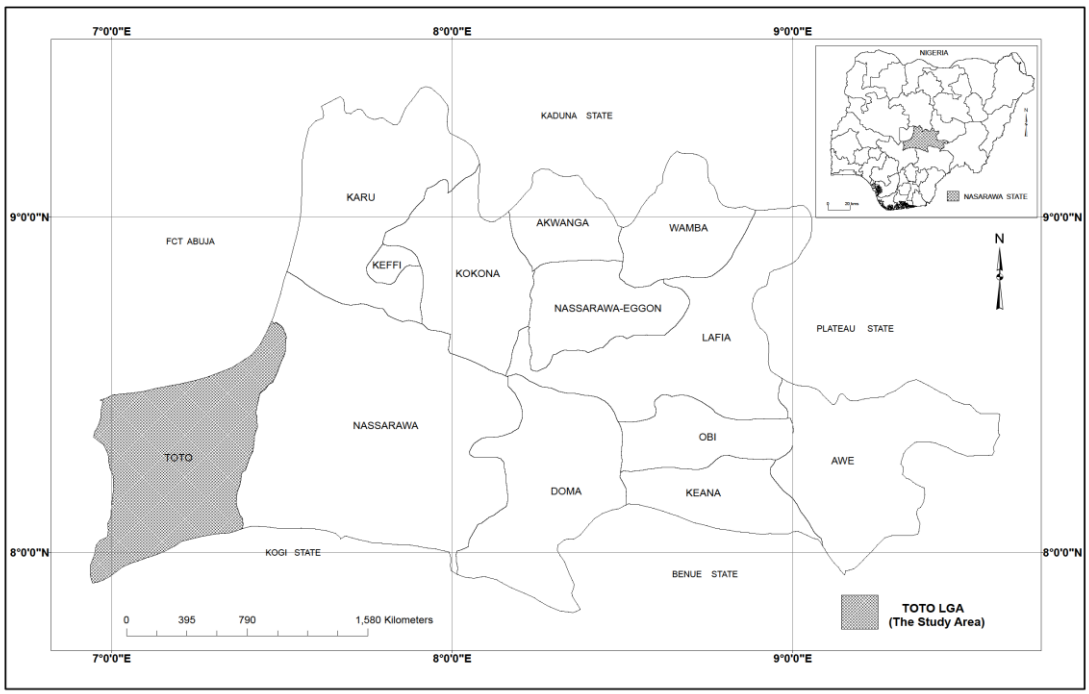

Figure 1. Toto LGA in Nasarawa State
Source: Dept. of Geography NDA Kaduna (2023)

Data Type and Sources

Landsat ETM + data

Landsat Enhanced Thematic Mapper+ (Landsat-7 ETM+) data of path and row 189/051, was downloaded from www.earthexplorer.com. The Landsat instrument consists of whisk broom system operated at an altitude of 705 km. Each Landsat Scene has an approximate extent of 183 _ 183 km extent, and a total of 405 scenes are captured every 24 hrs. Landsat imagery is made up of 8 bands with information obtained from the visible, shortwave to infrared region. Ideally, bands 1 and 2 contain information recorded within the visible region, while bands 3 and 4 are mainly information from the Near Infrared. Bands 5 and 7 contain information from the short-wave infrared. However, band 6 contains information from the thermal infrared, and band 8 is the panchromatic band.

Aster data

The Advanced Space-borne Thermal Emission and Reflection Radiometer (ASTER) Dem acquired on 25/12/2009 was downloaded from www.earthexplorer.com. The ASTER Global Digital Elevation Model (GDEM) Version 3 (ASTGTM) provides a global digital elevation model (DEM) of land areas on Earth at a spatial resolution of 1 arc second (approximately 30-meter horizontal posting at the equator). The ASTER instrument operated from a height of 705 km, has a recurrent cycle of 16 days, and can receive information within three regions of the electromagnetic spectrum (visible, short wave infrared, and thermal infrared).

Data Processing and Analytical Techniques

Band Rationing

The surface exposures of rocks and minerals are characterized by a significant high and low reflectance within certain regions of the electromagnetic spectrum. These discrepancies associated with reflectance spectral are invaluable tools for mapping alteration types using the band ratio methodology. According to Drury (1993) and Inzana *et al.* (2003), band ratio is computed by dividing the digital number of a given pixel in a particular band, by the digital number of that same pixel in another band. The resultant pixels with similar spectral characteristics to the material being mapped are often identified by their higher pixel values (Mars and Rowan, 2011). The application of band ratio using Landsat data for alteration mapping is restricted to the clay and iron altered minerals. Generally, the clay bearing minerals are characterized by a high reflectance on band 5 and a significantly low reflectance on band 7 Spectral attributes of ferrous and ferric iron minerals are characterized by high reflectance on band 5 and 3 and a corresponding low reflectance on band 4.

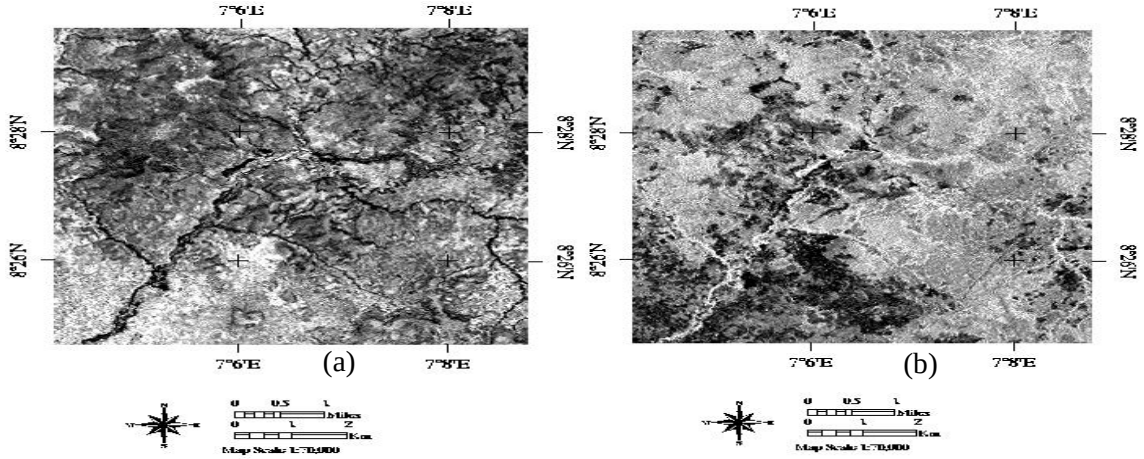

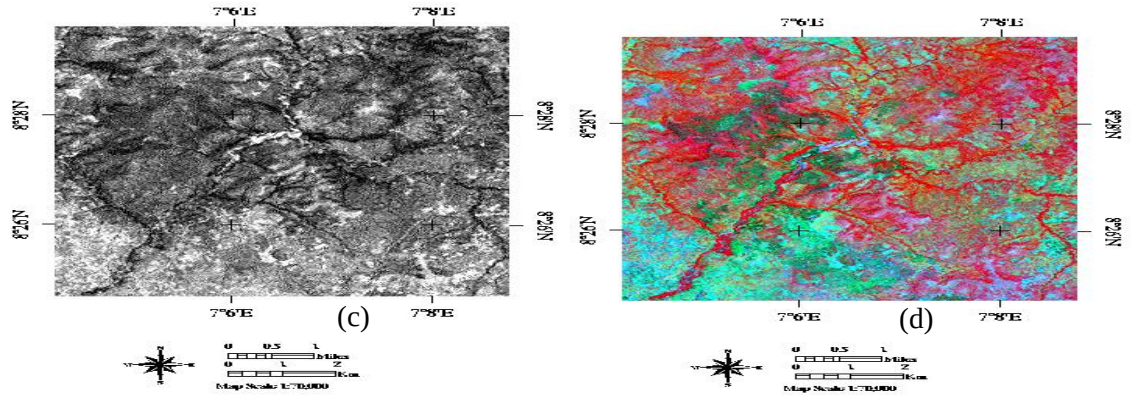

Figure 2: (a) Band Ratio 5/7 image (b) Band Ratio 5/4 (c) Band Ratio 3/1 (d) False colour composite

Principal Component Analysis (PCA)

Multispectral data in remote sensing often exhibit redundancy, resulting in spatial similarity among bands. Principal Component Analysis (PCA) can effectively address this issue by reducing data redundancy and projecting it onto a new set of uncorrelated axes. In the context of mineral exploration, PCA has been utilized to identify alteration patterns that may indicate mineralization in a specific area of interest. For example, in Landsat imagery, PCA has been applied to bands 1457 and 1345 to detect clay and iron alteration patterns, respectively. Certain bands, such as bands 3 and 7, are omitted to avoid mapping clay and iron-bearing alterations. In the case of ASTER imagery, PCA is commonly used to identify argillic, phyllic, and potassic alterations. Different combinations of bands are applied for mapping these alterations, such as bands 1,4,6,7 for argillic alteration, bands 1,3,5,6 for phyllic alterations, and bands 1,3,5,8 for potassic alteration. It is essential to accurately interpret the output PCA bands to analyze the data effectively well.

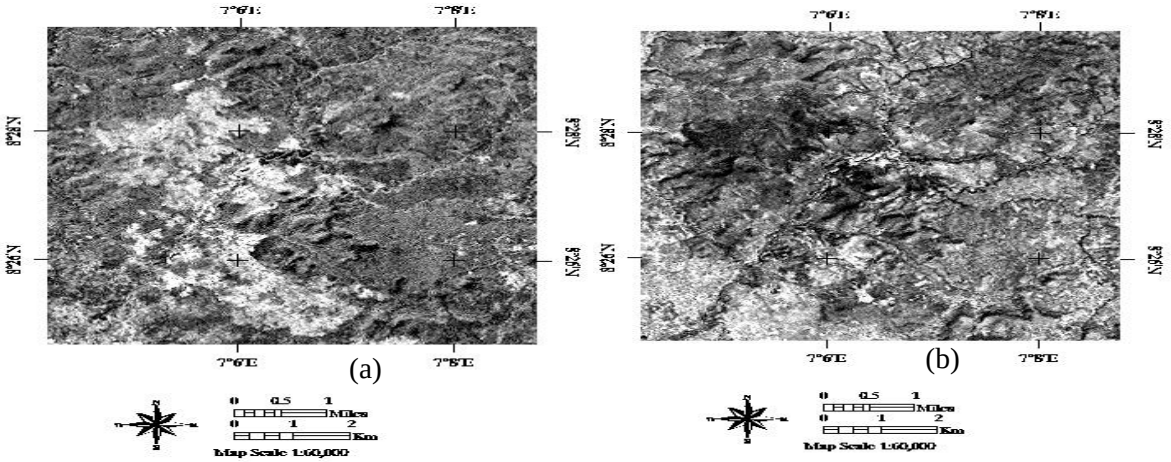

Figure 3: Principal component image (a) = PC4 image displaying clay minerals as light tone (b) PC$ image display iron minerals as light tone

Table 1: The Eigen vector loading for Iron mapping

Eigenvector	Band 1	Band 3	Band 4	Band 5
PC1	0.461376	0.582935	0.313271	0.590915
PC2	-0.471368	-0.137559	0.870108	0.042454
PC3	0.750503	-0.406999	0.360557	-0.375626
PC4	-0.041092	0.689650	0.121542	-0.712687

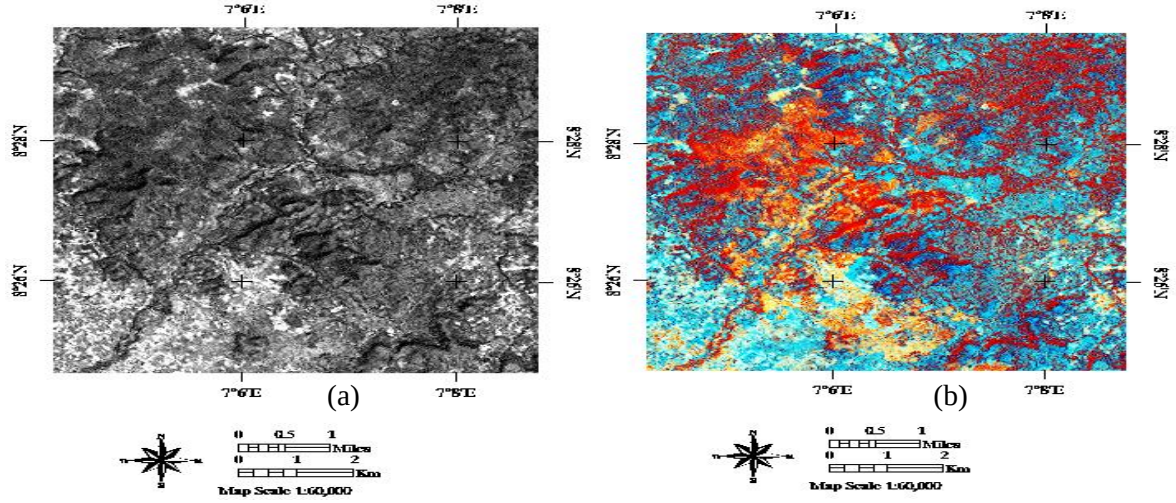

Figure 4: (a) H+F principal component image (b) Crosta image

Aeromagnetic Data Analysis

Aeromagnetic data was purchased from Nigerian Geological survey Agency and data processing was performed using Oasis montaj version 7.5. Total magnetic data was analyzed using analytical signal to enhance magnetic anomaly irrespective of direction and second vertical derivatives to enhanced shallow anomalies. On the analytical signal image major high anomalies are observed in the North West and South Eastern part of the study area (Figure). Other small anomalies are observed on the North Eastern part of the study area. On the second vertical derivative image, high anomalies are observed on the western and Eastern corridors of the study area (Figure 5).

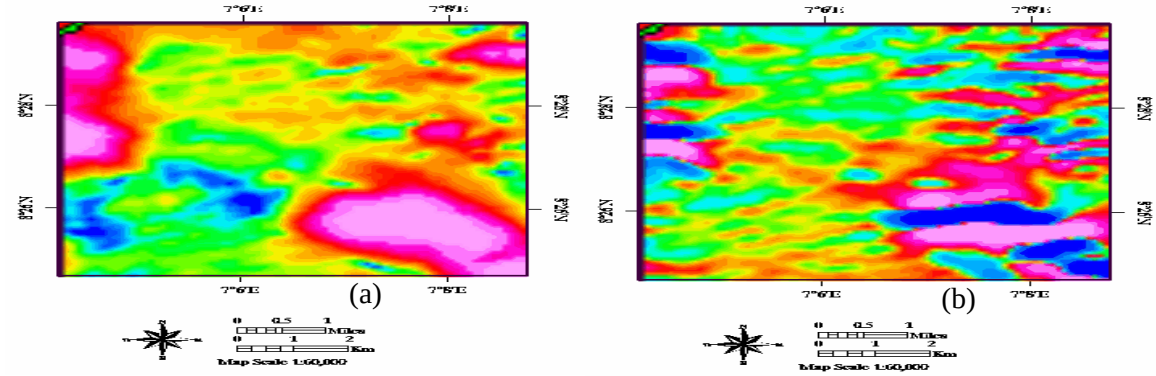

Figure 5: Showing the aeromagnetic maps of the study area

Lineament Analysis

Lineaments can be defined as natural crustal structures that may represent a zone of structural weakness (Massoud and Koike, 2006). On airborne or orbital remote sensing data, surface expression of geological structures such as fractures (faults and joints) and shear zones as well as foliations are shown in the form of lineaments (Semere and Woldai, 2006). According to Salau *et.al*, (2016),

positive straight lineaments may be interpreted as linear ridges, scraps, troughs and crater (Light tone). Negative straight lineaments represent joints, faults and shear zones (Dark tone). Mapping of geological lineaments is very important in the field of engineering solving especially for site selection (Dam construction), Seismic and land risk assessment, Mineral exploration, hot spring delineation, hydrogeologic research (Sabins, 1997). Lineaments were manually digitized from high resolution imagery, digital elevation model and geophysical imagery. Lineaments were super imposed on hydrothermal alteration imagery to map possible zones of mineralization (Figure).

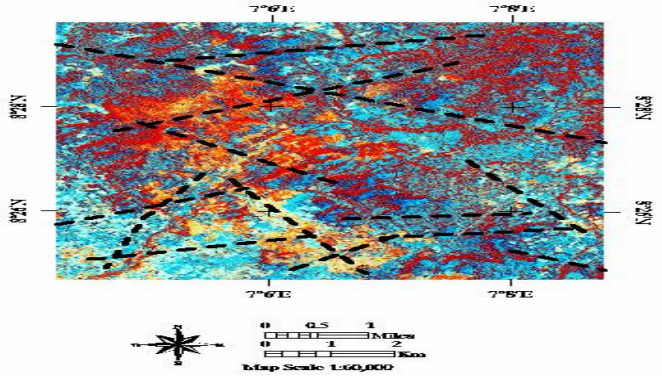

Figure 6: Showing the Lineaments superimposed on hydrothermal alteration map

Field Sampling Survey

The sampling approach used in the study involved conducting an orientation survey to determine optimal survey parameters for the entire concession area and prioritize specific areas. Undisturbed sites were selected, away from major contamination sources, and samples were taken approximately 30cm below the A horizon. Organic horizons and non-decomposed matter were removed, and precautions were taken to avoid cultural and wind-borne contamination. Soil samples weighing 200-400g were collected, properly labelled, and placed in clean plastic bags. No jewellery was worn during sample collection to prevent contamination. Samples were collected consistently at a depth of approximately 30cm below the A horizon, considering factors such as topography, soil moisture, and overburden characteristics in the survey area.

Field Work/Ground Truthing

The study area consists of three distinct lithologies: muscovite and quartz muscovite schist, feldspathic sandstone and siltstone, and marble. Within the schist belt, structures such as quartz veins were observed. The gold mineralization is primarily associated with these intruded quartz veins. Evidence of shearing was also observed within the schist belt, suggesting the area has undergone tectonic events. Stream sediments were collected along the curves of the stream and panned to concentrate the elemental content of the samples. Trenching and pitting were conducted at a depth of 30cm to obtain soil samples. Additionally, rock samples were collected from various locations to characterize the lithological units of the study area and determine their elemental composition.

Geochemical Sampling using the KXRF Analysis technique:

Kα X-ray Fluorescence (KXRF) is a geochemical analysis technique used in laboratories to determine the elemental composition of a sample. The process involves the excitation of atoms in the sample using X-rays, followed by the measurement of the resulting characteristic X-ray emissions. By examining the chemical makeup of samples, even minuscule quantities of elements can be identified, facilitating the recognition of the surface manifestation or "footprint" of the ore body via a systematically spaced sampling grid. The media sampled in this geochemical survey includes residual soil and whole rocks encountered during the systematic pitting process.

To implement this technique effectively in this study, the following step-by-step description of the KXRF analysis technique was applied:

i. Field sample collection and preparation: This involves collecting samples from the study area using materials and tools such as topographic maps, compasses, hand trowels,

sample bags, measuring tapes, diggers, and shovels. The sample of interest is collected and prepared for analysis. This may involve crushing, grinding, and homogenizing the sample to obtain a representative portion for testing. The sample is typically reduced to a fine powder to ensure uniformity and increase the surface area for analysis.

ii. X-ray Excitation: The prepared sample is placed in the sample chamber of the KXRF instrument. X-rays with specific energy levels are generated by an X-ray tube and directed towards the sample. These X-rays have sufficient energy to dislodge inner shell electrons of the atoms in the sample.

iii. X-ray Emission: When the X-rays interact with the atoms in the sample, the dislodged inner shell electrons are replaced by outer shell electrons. This transition releases energy in the form of characteristic X-rays. Each element in the sample emits X-rays at specific energy levels unique to that element.

iv. X-ray Detection: The emitted X-rays are collected using a detector, such as a solid-state detector or a gas proportional counter. The detector records the energy and intensity of the X-rays emitted by the sample. The X-ray spectrum obtained represents the elemental composition of the sample.

v. Calibration and Quantification: To determine the elemental composition accurately, calibration is performed using known reference standards with known elemental concentrations. The calibration process establishes the relationship between the X-ray intensities observed from the reference standards and the corresponding element concentrations. This calibration curve is then used to quantify the elemental concentrations in the sample.

vi. Data Analysis: This was carried out using the Kα X-ray Fluorescence (KXRF) Geochemical analysis technique to determine the elemental composition of various materials, including rocks, soils, sediments, and minerals. It is a non-destructive method that relies on the principle of X-ray fluorescence. In KXRF analysis, a high-energy X-ray beam is directed at the sample, causing the atoms in the sample to emit characteristic X-rays. The collected X-ray data is analyzed using specialized software or algorithms. The software compares the energy peaks observed in the sample spectrum with those of the calibration standards to identify the elements present and their respective concentrations. The results are typically reported as weight percentages or parts per million (ppm) for each detected element.

vii. Quality Control: To ensure the accuracy and reliability of the results, quality control measures are implemented. This may include running replicate measurements, analyzing certified reference materials alongside the samples, and performing instrument performance checks regularly.

viii. Interpretation and Reporting: The final step involves interpreting the results and reporting the elemental composition of the sample. The obtained data can be used for various applications, such as geological exploration, environmental monitoring, archaeological studies, and material characterization.

To ensure accuracy and comparability of results, the International Organization for Standardization (ISO) has established a world measurement standard for X-ray fluorescence analysis, including KXRF. The ISO standard for X-ray fluorescence analysis is ISO 16732-1:2012, titled "Geological Analysis - Guidelines for X-ray Fluorescence Analysis of Geological Samples - Part 1: General Requirements." ISO 16732-1 provides guidelines for the preparation of geological samples. Adhering to this standard helps to ensure that results obtained using KXRF are reliable, reproducible, and compatible across different laboratories.

RESULTS

This section presents the results from the Kα X-ray Fluorescence (KXRF) Geochemical analysis conducted to determine the elemental composition of a sample. The study provides insights into the oxide composition (%) of the different analysed samples labelled as ST1A, ST2, ST3, ST4, and STV5. Each sample is analyzed for the presence of oxides. Table 2 presents the result of Oxide composition (%) of the samples.

Table 2: Oxide Composition (in percentage) of Samples labelled ST1A - STV5

Oxide composition (%)	ST1A	ST2	ST3	ST4	STV5
Sio2	84.01	84.44	71.13	83.55	80.40
Tio2	3.72	2.05	9.73	2.63	5.09
Al2o3	5.44	5.61	6.14	6.33	7.17
Fe2o3	4.21	4.92	9.75	4.65	4.06
Cao	0.18	0.18	0.27	0.17	0.052
Mgo	0.014	0.013	0.034	0.08	0.011
Na2o	0.32	0.31	0.679	0.32	<0.001
K2o	0.51	0.41	0.23	0.093	<0.001
Mno	0.15	0.14	0.23	0.093	0.01
V2O5	<0.001	0.004	<0.001	<0.001	<0.001
Cr3O3	0.032	0.011	<0.001	0.021	0.022
CuO	0.012	0.013	0.018	0.012	0.017
ZnO	0.004	ND	0.008	ND	0.007
Ga2O3	ND	ND	ND	ND	0.008
As2O3	0.003	ND	0.001	0.003	ND
Rb2O	ND	0.005	ND	0.005	ND
ZrO2	0.169	0.072	0.838	0.130	1.20
Nb2O5	ND	ND	ND	ND	0.027
BaO	0.10	0.091	0.20	0.10	0.30
PbO	0.030	0.030	0.050	0.040	0.035
L.O.I	1.10	1.70	0.60	1.30	1.50

Results from Table 2 show that SiO2 (silicon dioxide) is the most abundant oxide in all the samples, ranging from 71.13% to 84.44%. The variation in SiO2 content suggests differences in the mineral composition or geological origin of the samples. The content of TiO2 (titanium dioxide) varies from 2.05% to 9.73%. The higher TiO2 content in ST3 indicates a potential presence of titanium-bearing minerals in that sample. Al2O3 (aluminum oxide) presents a percentage of Al2O3 which is relatively consistent across all samples, ranging from 5.44% to 7.17%. This suggests a common source or similar mineralogy for these samples. The content of Fe2O3 (iron(III) oxide) ranges from 4.06% to 9.75%. Higher Fe2O3 content may indicate the presence of iron-rich minerals or geological processes related to iron oxidation. While CaO (calcium oxide), MgO (magnesium oxide), Na2O (sodium oxide), and K2O (potassium oxide) present in small amounts (<1%). Their concentrations are relatively low and consistent across the samples, indicating minor contributions from calcium, magnesium, sodium, and potassium-bearing minerals. The content of MnO (manganese oxide) ranges from 0.01% to 0.23%.

Oxide Composition (in percentage) of different Samples labelled as STV 10 - VR

Table 3 presents the oxide composition (%) of samples labelled as STV 10, GL 01, GL 02, GL 03, and VR.

Table 3: Oxide Composition (in percentage) of Samples labelled as STV 10 - VR

Oxide composition (%)	STV 10	GL 01	GL02	GL03	VR
Sio2	94.01	92.13	90.08	68.70	80.49
Tio2	0.164	0.950	2.33	13.70	0.818
Al2o3	3.55	3.48	3.19	10.20	5.22
Fe2o3	0.931	1.938	2.527	10.20	3.875
Cao	0.049	0.22	0.11	0.079	0.46
Mgo	0.015	0.023	0.025	0.01	0.11
Na2o	0.021	0.11	<0.001	<0.001	0.98
K2o	0.059	0.14	<0.001	<0.001	1.32
Mno	0.010	0.044	0.070	0.18	0.092

V2O5	<0.001	<0.001	<0.001	<0.001	0.028
Cr3O3	0.018	<0.001	0.026	<0.001	0.054
NiO	0.004	ND	0.004	ND	0.008
CuO	0.008	0.012	0.009	ND	0.024
ZnO	ND	ND	ND	0.032	0.009
Ga2O3	ND	ND	0.001	ND	0.010
As2O3	0.009	0.006	0.005	0.004	ND
Rb2O	ND	ND	ND	ND	0.017
SrO	ND	ND	ND	ND	0.019
ZrO2	0.033	0.025	0.308	0.026	0.032
Nb2O5	ND	ND	ND	0.77	ND
BaO	ND	ND	0.094	0.77	0.06
HfO2	ND	ND	ND	0.10	ND
PbO	0.017	0.027	0.015	0.032	0.076
L.O.I	1.10	0.90	1.20	1.30	6.30

The results presented in Table 3 display the variation in elemental composition among the analysed samples using KXRF analysis. SiO2 (silicon dioxide) content ranges from 68.70% to 94.01%, indicating significant differences in mineral composition or geological origin. TiO2 (titanium dioxide) content varies considerably, with GL03 showing a high concentration, suggesting the presence of titanium-rich minerals in that sample. The percentage of Al2O3 (aluminum oxide) remains relatively consistent across the samples, except for GL03, which exhibits a higher content. Fe2O3 (iron(III) oxide) content ranges from 0.931% to 10.20%, with GL03 and VR showing higher concentrations, potentially indicating the presence of iron-rich minerals or iron oxidation processes.

Oxide Composition (in percentage) of different Samples labelled as VRV-SI – ST04

Table 4 presents the oxide composition (%) of samples labelled as VRV-S1, VRII-S2, PIT S1A, PIT 02, and ST04

Table 4: Oxide Composition (in percentage) of Samples labelled as VRV-SI - ST04

Oxide composition (%)	VRV-S1	VRII-S2	PIT S1A	PIT 02	ST04
Sio2	2.72	86.84	60.43	87.26	95.58
Tio2	4.38	1.24	2.24	0.599	0.009
Al2o3	8.40	4.79	11.88	3.67	2.81
Fe2o3	66.49	3.272	9.63	2.226	0.433
Cao	0.94	0.27	0.63	0.21	0.042
Mgo	0.17	0.013	0.07	0.012	0.01
Na2o	1.59	0.66	2.14	0.45	<0.001
K2o	1.96	0.94	1.70	0.75	<0.001
Mno	0.25	0.057	0.083	0.078	0.014
V2O5	0.06	0.01	0.087	0.001	<0.001
Cr3O3	0.095	0.025	0.041	0.005	0.014
NiO	ND	ND	ND	ND	0.005
CuO	0.22	0.009	0.039	0.016	0.007
ZnO	0.11	ND	0.032	ND	ND
Ga2O3	0.04	0.001	0.003	0.003	ND
As2O3	ND	0.002	ND	ND	0.007
Rb2O	0.23	0.011	0.047	0.012	ND
SrO	0.24	ND	0.055	0.013	ND
ZrO2	0.63	0.077	0.12	0.022	ND
BaO	ND	0.02	0.07	0.04	ND
Ta2O5	0.10	0.018	ND	ND	ND
PbO	0.53	0.041	ND	0.032	0.038
L.O.I	10.20	1.70	10.70	4.60	1.03

The results presented in Table 3, highlight the variations in elemental composition among the analyzed samples. SiO2 (silicon dioxide) content varies significantly, ranging from 2.72% to 95.58%. The highest SiO2 content in ST04 suggests a silica-rich composition, while

lower values in VRV-S1 and VRII-S2 indicate different mineralogical compositions. TiO2 (titanium dioxide) content ranges from 0.009% to 4.38%, with PIT S1A showing higher concentrations, indicating the potential presence of titanium-bearing minerals in that sample. Al2O3 (aluminum oxide) exhibits variation across the samples, ranging from 2.81% to 11.88%, with PIT S1A displaying a higher content, suggesting a distinct mineralogical composition compared to other samples.

Fe2O3 (iron(III) oxide) shows a wide range of variation, from 0.433% to 66.49%, with the highest Fe2O3 content observed in VRV-S1, indicating the presence of iron-rich minerals in that sample. CaO (calcium oxide), MgO (magnesium oxide), Na2O (sodium oxide), and K2O (potassium oxide) are present in small amounts (<3%) in most samples, except for VRV-S1 and PIT S1A, where their concentrations are relatively higher.

Oxide Composition (in percentage) of different Samples labelled as ST05B - HNVSI

Table 5 presents the oxide composition (%) of samples labelled as ST05B, STV S9, HN IV SI, VR IV SI and HN V S1.

Table 5: Oxide Composition (in percentage) of Samples labelled as ST05 – HN VSI

Oxide composition%	ST05B	STV S9	HN IV S1	VR IV S1	HN V S1
Sio2	1.18	88.01	1.45	2.67	96.26
Tio2	1.20	0.527	<0.001	3.32	0.042
Al2o3	4.60	3.04	4.39	6.11	1.66
Fe2o3	4.21	2.55	79.90	72.76	0.899
Cao	81.55	0.653	0.070	0.21	0.21
Mgo	0.11	0.13	0.02	0.008	0.014
Na2o	0.02	0.55	<0.001	1.09	0.09
K2o	0.23	0.75	<0.001	1.71	0.11
Mno	0.26	0.248	<0.001	0.27	0.045
V2O5	0.01	0.006	<0.001	0.03	<0.001
Cr3O3	0.068	0.024	0.046	0.069	0.025
NiO	ND	ND	ND	ND	0.006
CuO	0.089	0.016	0.038	0.18	0.011
ZnO	0.073	0.005	0.13	0.06	ND
As2O3	ND	0.002	ND	ND	0.006
Rb2O	0.02	0.010	ND	0.21	ND
SeO2	ND	ND	ND	ND	0.008
SrO	ND	0.015	0.062	ND	ND
ZrO2	0.45	0.025	ND	1.10	ND
BaO	0.61	0.05	ND	0.66	ND
PbO	1.43	0.191	0.26	0.64	0.030
L.O.I	7.90	3.20	13.70	8.90	0.60

Results from Table 5 reveal variations in the elemental composition of the analyzed samples. SiO2 (silicon dioxide) content ranges from 1.18% to 96.26%, with ST05B having the lowest and HN V S1 having the highest content. These variations indicate differences in mineralogical composition and potential geological origins of the samples. TiO2 (titanium dioxide) content ranges from <0.001% to 3.32%, with VR IV S1 showing a relatively higher concentration, suggesting the presence of titanium-bearing minerals in that sample. Al2O3 (aluminum oxide) varies from 1.66% to 6.11%, with HN V S1 having the lowest and VR IV S1 having the highest content. These variations reflect differences in mineralogical composition and potential aluminum-rich minerals in the samples. Fe2O3 (iron(III) oxide) content exhibits significant variation, ranging from 0.899% to 79.90%, with HN IV S1 having the highest concentration, indicating a high presence of iron-bearing minerals in that sample.

Oxide Composition (in percentage) of Samples labelled as ST1A - HNVSI

Table 6 presents the concentrations of various elements (in parts per million or ppm) in

different samples labelled as ST1A, ST3, ST04, STV10, GL01, GL02, GL03, VR II S2, ST04, STVS9, and HNVS1. The elements analyzed include (arsenic), Cu (copper), Pb (lead), Zn (zinc), and Mn (manganese).

Table 6: Oxide Composition (in percentage) of Samples labelled as ST1A - HNVSI

SAMPLE ID	As	Cu	Pb	Zn	Mn
ST1A	0.003	0.012	0.030	0.004	0.15
ST3	0.001	0.18	0.050	0.008	0.23
ST04	0.003	0.014	0.040	ND	0.093
STV10	0.009	0.008	0.017	ND	0.010
GL01	0.006	0.012	0.027	ND	0.044
GL02	0.005	0.009	0.015	ND	0.070
GL03	0.004	ND	0.032	0.032	0.18
VR II S2	0.002	0.009	0.041	ND	0.05
ST04	0.007	0.07	0.038	ND	0.014
STVS9	0.002	0.016	0.191	0.005	0.248
HNVS1	0.006	0.011	0.031	ND	0.045

Results from Table 6 show Arsenic (As) concentrations ranging from 0.001 ppm to 0.009 ppm in the samples. Arsenic is a toxic element, and its presence in the environment can have significant health implications. Monitoring and assessing its concentration in different samples help in evaluating potential environmental risks and human exposure. Copper (Cu) concentrations vary from <0.01 ppm to 0.18 ppm in the samples. Copper is an essential element in various biological processes and has industrial applications. Monitoring copper concentrations is important for assessing its potential environmental impact and understanding its sources. Lead (Pb) presents a concentration range from 0.015 ppm to 0.191 ppm in the samples. Lead is a highly toxic element, and its presence in the environment can pose serious health risks, particularly to children. Monitoring and controlling lead levels are crucial for ensuring environmental and public health. Zinc (Zn): The concentrations of zinc range from ND (not detected) to 0.032 ppm in the samples. Zinc is an essential element for living organisms and has various industrial applications. Monitoring its concentration helps in understanding environmental sources and assessing its potential effects. Manganese (Mn) ranged from 0.01 ppm to 0.248 ppm in the samples. Manganese is an essential element, but elevated concentrations can be harmful. Monitoring manganese levels is important for assessing its environmental impact and potential health risks.

DISCUSSION

The XRF analysis of various sample ST1A, ST3, ST04, STV10, GL01, GL02, GL03, VRII S2, STO4, STVS9, HNVS1 in most profiles generally have the highest concentration (response) of key pathfinder elements (As, Cu, Pb, Zn, Mn). Assessment of the geochemical data indicates that Fe as iron oxide/oxyhydroxide has an important influence on pathfinder element geochemistry in the study area samples. This is indicated by moderate to strong positive correlation between Fe and these elements in the total data set and the individual profile distribution patterns. This influence is particularly marked in the medium and coarse size fractions, consistent with the observed presence of iron oxide/oxyhydroxides in larger aggregates and ferruginous pedogenic nodules, especially at HNVS1. This association with iron oxide/oxyhydroxide highlights the importance of observing and noting the presence of ferruginous concentrations, aggregates and nodules in the soil profiles. Result from the study also shows that arsenic generally shows a selective concentration in some samples. Arsenic is major pathfinder of Au mineralization. After arsenic, copper is probably the most useful of the major pathfinder elements.

The presence of higher MnO content in ST3 (Table 1) indicates the likely presence of manganese-bearing minerals in that sample. Elements, including V2O5, Cr3O3, CuO, ZnO,

Ga_2O_3, As_2O_3, Rb_2O, ZrO_2, Nb_2O_5, BaO, and PbO, are found in trace amounts or below the detection limit (ND) in some samples. Their low concentrations suggest minor contributions or absence of corresponding elements in the analyzed samples. Additionally, the Loss on Ignition (L.O.I) values, ranging from 0.60% to 1.70%, indicate the presence of volatile components, such as water or organic matter, in the samples. These variations in oxide concentrations can aid in identifying potential mineralogical differences between the samples and provide insights into their geological origin or formation processes.

Most samples (Table 2) contain CaO, MgO, Na_2O, and K_2O in small amounts (<1%), except for GL03 and VR, which have higher Na_2O and K_2O contents, suggesting an additional contribution from sodium- and potassium-rich minerals. Similarly, MnO, V_2O_5, Cr_3O_3, NiO, CuO, ZnO, Ga_2O_3, As_2O_3, Rb_2O, SrO, ZrO_2, Nb_2O_5, BaO, HfO_2, and PbO are present in trace amounts or below the detection limit (ND) in some samples, indicating minor contributions or their absence. The Loss on Ignition (L.O.I) values, ranging from 0.90% to 6.30%, indicate the presence of volatile components, such as water or organic matter, in the samples. Notably, VR stands out with a significantly higher L.O.I, suggesting a higher content of volatile substances in that particular sample.

In some samples (Table 3), trace amounts or concentrations below the detection limit (ND) were detected for elements such as MnO (manganese oxide), V_2O_5 (vanadium pentoxide), Cr_3O_3 (chromium(III) oxide), NiO (nickel(II) oxide), CuO (copper(II) oxide), ZnO (zinc oxide), Ga_2O_3 (gallium oxide), As_2O_3 (arsenic trioxide), Rb_2O (rubidium oxide), SrO (strontium oxide), ZrO_2 (zirconium dioxide), BaO (barium oxide), Ta_2O_5 (tantalum pentoxide), and PbO (lead(II) oxide). This indicates minor contributions or the absence of these elements in those particular samples. The Loss on Ignition (L.O.I) values range from 1.03% to 10.70%, indicating the presence of volatile components such as water or organic matter in the samples. Notably, PIT S1A and VRV-S1 exhibit higher L.O.I values, suggesting a higher content of volatile substances in those samples.

Regarding CaO (calcium oxide), MgO (magnesium oxide), Na_2O (sodium oxide), and K_2O (potassium oxide), (Table 5) they are present in varying amounts. Particularly, ST05B shows a notably high CaO content, suggesting a calcium-rich composition. On the other hand, trace amounts of MgO, Na_2O, and K_2O indicate their minor contributions or absence in some samples. MnO (manganese oxide), V_2O_5 (vanadium pentoxide), Cr_3O_3 (chromium(III) oxide), NiO (nickel(II) oxide), CuO (copper(II) oxide), ZnO (zinc oxide), As_2O_3 (arsenic trioxide), Rb_2O (rubidium oxide), SeO_2 (selenium dioxide), SrO (strontium oxide), ZrO_2 (zirconium dioxide), BaO (barium oxide), and PbO (lead(II) oxide) are also present in trace amounts or below the detection limit (ND) in some samples, suggesting minor contributions or absence of corresponding elements. Loss on Ignition (L.O.I) values range from 0.60% to 13.70%, with HN IV S1 showing the highest L.O.I, indicating a higher content of volatile substances in that particular sample.

The elevated levels of certain elements in several samples (Table 6) suggest the potential presence of mineral deposits in the area. For example, high concentrations of arsenic (As) may indicate gold, copper, or polymetallic sulfide deposits, while increased copper (Cu) concentrations are associated with copper mineralization. Moreover, lead (Pb) concentrations suggest lead-zinc or lead-silver deposits, while significant zinc (Zn) concentrations indicate zinc-lead or zinc-copper deposits. Higher manganese (Mn) levels may suggest the potential for manganese mineralization. These findings are in line with the study conducted by Moumouni et al. (2016) on marble deposits in the Muro-Obugu-Panda area of Toto, where variations in CaO, Fe_2O_3, Al_2O_3, MgO, and SiO_2 content were observed. The correlation between Fe and pathfinder elements highlights the influence of iron oxide/oxyhydroxide on their geochemistry, particularly in larger aggregates and ferruginous nodules. It is essential to consider the presence of ferruginous concentrations in soil profiles for accurate interpretation. Additionally, the selective concentration of arsenic, serving as a major pathfinder for gold mineralization, supports the presence of gold in the Toto schist belt. The existence of multiple

pathfinder elements further strengthens the indication of gold mineralization in the area

CONCLUSION AND RECOMMENDATIONS

The exploration of the geochemistry of gold mineralization in Toto Local Government Area, Nasarawa State, Nigeria has provided valuable insights into the presence and potential of gold deposits in the region. The geochemical analysis of samples has revealed the concentrations of pathfinder elements such as arsenic, copper, lead, zinc, and manganese, which are commonly associated with gold mineralization. The high levels of these elements in certain samples indicate the possibility of underlying mineral resources and highlight areas of interest for further exploration. The findings of this study therefore, provides a foundation for informed decision-making, sustainable management of mineral resources, and future exploration and exploitation of gold deposits in the region. Based on the geochemistry of gold mineralization in Toto Local Government Area, Nasarawa State, Nigeria, the following recommendations are proposed:

i. Conduct Detailed Geochemical Surveys: Perform extensive surveys to gather comprehensive data on the distribution and concentration of gold and associated elements. This will aid in identifying potential zones of gold mineralization and understanding the geological factors influencing gold deposition.
ii. Analyze Samples and Conduct Laboratory Testing: Utilize appropriate laboratory techniques to analyze collected samples accurately. This analysis will enable the determination of gold content and the presence of other valuable minerals, contributing to the assessment of economic viability.
iii. Perform Geological Mapping and Structural Analysis: Carry out detailed mapping and analysis of the study area to identify geological formations, structures, and alteration zones associated with gold mineralization. This information will guide exploration efforts and enhance understanding of the geological controls on gold deposition.
iv. Integrate Remote Sensing and Geophysical Techniques: Incorporate remote sensing data and geophysical methods to identify potential areas of interest for gold mineralization. This can involve analyzing satellite imagery, aerial photographs, magnetic surveys, and gravity surveys to detect subsurface structures and anomalies related to gold deposits.

REFERENCES

Drury S. A., (1993). Image Interpretation in Geology, 2nd ed. xi + 283 pp. London, Glasgow, New York, Tokyo, Melbourne, Madras: Chapman ' Hall). ISBN 0 412 48880 9. Published online by Cambridge University Press

Masoud and Koike, (2006). Integrated remote sensing data utilization for investigating structural and tectonic history of the Ghadames Basin, Libya. *International Journal of Applied Earth Observation and Geoinformation* 13(5):778-791.

Moumouni, A., Goki, N. and Chaanda, M. (2016). Geological Exploration of Marble Deposits in Toto Area, Nasarawa State,Nigeria. *Natural Resources*, (7): 83-92.

Obaje, N. G., and Mallo, S. J. (2010). Geochemistry and alteration mapping of the Toto area, Nasarawa State, Nigeria. *Journal of Mining and Geology*, 46 (2):215-226.

Okonkwo, C. C., and Dada, S. S. (2020). Gold Mineralization Potential in Toto Area, Nasarawa State, Nigeria: Insight from Remote Sensing and GIS Techniques. Geology, Ecology, and Landscapes, 4(3): 218-230

Oyinloye, A. O., and Oyinloye, R. O. (2017). Petrography and Geochemistry of the Precambrian Gneissic Rocks from Toto, Nasarawa State, Nigeria. *Global Journal of Geological Sciences*, 15(1): 45-52

Sabins, F.F., 1999. Remote sensing for mineral exploration. Ore. Geol. Rev. 14 (3–4): 157 - 183.

Salau, S.L., Danbatta, U.A., Agunleti, Y.S., (2016). The Interpretation of Aeromagnetic and Satellite Imagery for Structures in Coincident with Gold Mineralization in Anka Schist Belt, Northwestern Nigeria. *IOSR J. Applied Geol*. Geophys. 4 (5): 29–34.

Semere, S and Woldai, G. (2006): Lineament characterization and their tectonic significance using Landsat TM data and field studies in the central highlands of Eritrea November 2006 *Journal of African Earth Sciences* 46(4):371-378